



EFFECT OF NON-METALLIC INCLUSIONS ON FORMATION OF STRUCTURE OF THE WELD METAL IN HIGH-STRENGTH LOW-ALLOY STEELS

V.V. GOLOVKO and I.K. POKHODNYA

E.O. Paton Electric Welding Institute, NASU,
11 Bozhenko Str., 03680, Kiev, Ukraine. E-mail: office@paton.kiev.ua

Investigated was the possibility of using the oxide metallurgy approaches providing for control of the amount, distribution and morphology of the inclusions in metal melts, which affect conditions for formation of microstructure of the weld metal. It was shown that increase in the content of the fine-grained secondary phase can be achieved by varying the content of the fine carbide phase in structure of the weld metal. A high density of distribution of the 0.3–1.0 μm inclusions containing titanium or zirconium oxides leads to formation of the bainitic structure, whereas the decreased content of carbon in metal and narrowing of the range of bainitic transformations limit the probability of formation of the upper bainite microstructure. It was found that to provide the microstructure characterised by a combination of high values of strength, ductility and toughness it is necessary to form inclusions of a certain composition, size and distribution density in the weld metal. This can be achieved by using the oxide metallurgy methods, which provide for addition of a certain amount of refractory inclusions to the weld pool, limitation of its oxygen content and selection of the deoxidation system, as well as of the required temperature range of intermediate transformations based on the TTT-diagrams and welding thermal cycle. 12 Ref., 9 Tables, 13 Figures.

Keywords: *welding, low-alloy steels, oxide metallurgy, welds, non-metallic inclusions, alloying, microstructure, mechanical properties*

High-strength low-alloy (HSLA) steels have been receiving an increasingly wider acceptance in fabrication of metal structures during the last decades. Along with expansion of the scopes of consumption of this class of steels, we can note increasing requirements to the level of their mechanical properties, brittle fracture resistance and cost effectiveness. For example, a growing consumption of the natural gas by developed countries dictates increase in the working pressure of a transported gas from 55–75 to 100 or more, the growth of which in pipelines made from steels of strength category K60 (X70) leads to increase in metal intensity and specific costs. This is accompanied by increase in the level of requirements to operating safety, reliability and service life of pipelines, which in turn requires increase in impact toughness and brittle fracture resistance, as well as improvement of weldability of the said steels.

Transition from steels of strength categories K60 (X70) to steels K65 (X80) and stronger required revision of the principles of alloying and microalloying them from the metal science standpoints. Providing the required level of strength of sheet and plate products in a combination with other most important indices of mechanical prop-

erties ($\delta_5 > 22\%$, $KCV > 130 \text{ J/cm}^2$, and content of tough components in fractures of drop-weight test specimens $> 95\%$ at -20°C) is possible only in transition from the ferritic-pearlitic structure to the other structural state of a material, i.e. steels with the fine ferritic-bainitic structure [1, 2].

To ensure the required level of performance of welded metal structures, chemical and structural compositions, as well as mechanical properties of the weld metal should correspond to those of the base metal. The problem of formation of the weld metal with the ferritic-bainitic structure can be solved by using the possibilities offered by oxide metallurgy [3, 4].

The necessary condition for formation of the high-toughness fine structure of the type of acicular ferrite is the presence of a certain amount of non-metallic inclusions (NMI) in the weld metal [5, 6]. It should be noted that inclusions up to $1 \mu\text{m}$ in size, which contain titanium compounds, are most efficient in this respect [7–9].

The use of the oxide metallurgy approaches allows affecting the processes of initiation and growth of structural components by varying the composition, content and sizes of NMI [10, 11]. Investigation of the effect of NMI on the secondary microstructure was carried out on specimens of the weld metal of low-alloy steel of strength category K60 alloyed with carbon, manganese and silicon, with an adjustable content of oxygen and microalloyed with titanium. The welds were



Table 1. Chemical composition of metal of the investigated welds, wt.%

Weld designation	C	Si	Mn	Ni	Mo	Ti	Cr	Al	S	P	O
Ti-1	0.078	0.437	0.43	0.22	0.19	0.027	0.24	0.012	0.008	0.009	0.101
Ti-2	0.073	0.227	0.48	0.24	0.19	0.084	0.25	0.019	0.007	0.010	0.054
Ti-3	0.075	0.181	0.54	0.23	0.19	0.127	0.25	0.028	0.006	0.009	0.032
Ti-4	0.125	0.557	0.47	0.22	0.17	0.130	0.23	0.029	0.011	0.008	0.102
Ti-5	0.083	0.389	0.51	0.24	0.18	0.244	0.26	0.039	0.008	0.010	0.030
Ti-6	0.118	0.217	0.52	0.21	0.16	0.297	0.22	0.054	0.007	0.008	0.022

Table 2. Mechanical properties of metal of the investigated welds

Weld designation	σ_t , MPa	$\sigma_{0.2}$, MPa	δ_5 , %	ψ , %	KCV, J/cm ² , at T, °C		
					20	0	-20
Ti-1	597.5	437.7	23.15	58.8	62.4	42.9	23.7
Ti-2	603.5	443.4	23.5	67.7	64.3	40.8	19.0
Ti-3	665.9	527.2	18.8	66.9	43.3	20.9	13.8
Ti-4	807.3	664.2	17.6	66.0	22.2	16.7	13.0
Ti-5	769.0	673.3	17.5	68.9	28.5	13.8	16.0
Ti-6	634.0	488.9	20.6	59.8	49.6	18.3	13.9

made by the method of submerged-arc welding (welding heat input – about 33.4 kJ/cm). In this case the main part of oxygen transfers to the weld pool through the slag phase, as the distribution of oxygen between the slag and pool is determined by a ratio of the activity of oxygen in the slag (a_O) to the activity of oxygen in the weld pool metal [a_O]. Considering that the content of oxygen in metal is low and the [a_O] value is close to one, the transition of oxygen depends only on (a_O).

Chemical composition of metal of the investigated welds is given in Table 1, and its mechanical properties are given in Table 2.

Results of dilatometric investigations of the weld metal conducted by using the «Gleeble» high-speed dilatometer are shown in Figure 1. Composition of the microstructure components and their sizes were determined by using optical microscope «Neophot 30» (Table 3).

It was found that growth of the content of titanium in the weld metal is accompanied by increase in temperature of the finish of bainitic transformation B_f and decrease in the $\gamma \rightarrow \alpha$ transformation temperature range. Proportion of the titanium and oxygen in the weld metal affects the balance between the content of the inclusions above 1 μm in size consisting primarily of oxides

(Figure 2)*, and that of the inclusions less than 1 μm in size consisting of carbides (Figure 3). Increase in the content of fine carbides leads to increase in the content of upper bainite in the secondary structure of the weld metal (see Table 3). This causes increase in strength and decrease in impact toughness of the weld metal (see Table 2) due to an increased brittleness of the given structural component.

Alloying of the weld metal with titanium allows the size of the ferritic grains to be substan-

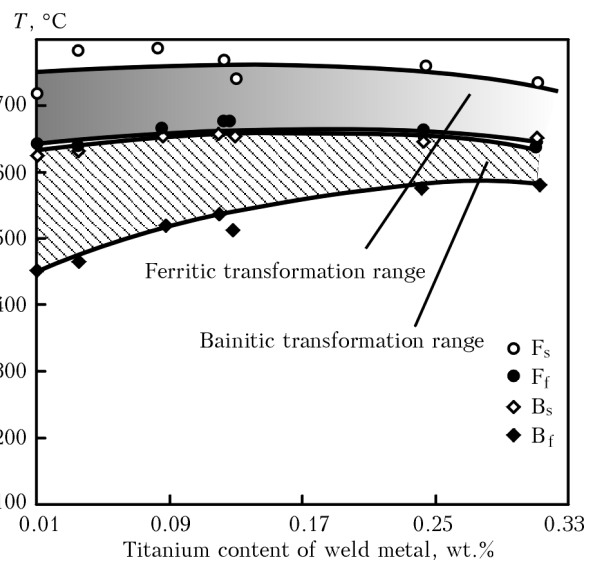


Figure 1. Dependence of temperature range of structural transformations in metal of the investigated welds on the titanium content: F_s , F_f – start and finish of ferritic transformation; B_s , B_f – start and finish of bainitic transformation

* The pictures in Figures 2 and 3 were obtained by Prof. V.N. Tkach by using scanning electron microscope EVO-50.

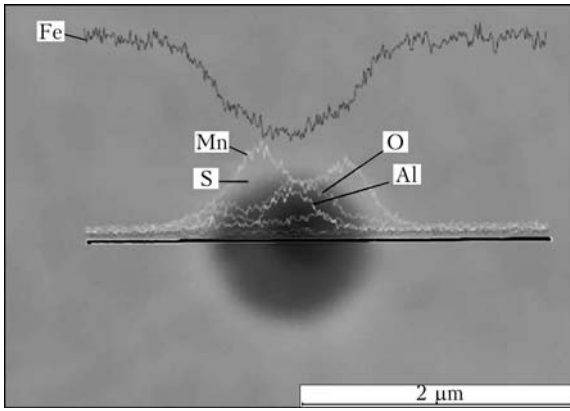


Figure 2. Morphology and composition of NMI more than 1.5 μm in size

of the effect of precipitation hardening on the formation of mechanical properties of the weld metal, on the other hand (Table 4). The effect of solid solution hardening of ferrite substantially increased in the Ti-6 weld metal.

Fine inclusions up to 1 μm in size have a core consisting of aluminium and titanium oxides, as well as an external cubic fringe with a high content of titanium nitrides (see Figure 3). Coarser inclusions consist of complex-composition oxides with manganese sulphide precipitates located on their surfaces (see Figure 2).

tially decreased (see Table 3). Increasing the content of the fine carbide phase in the weld metal alloyed with titanium leads to growth of the α-phase nucleation centres and refining of the ferritic grains, on the one hand, and to enhancement

Increase in the content of carbide inclusions in the weld metal led to refining of ferritic grains and increase in the density of distribution of the grain boundaries. In this case it is the grain boundaries that acted as the most probable, in terms of energy, centres of growth of the ferritic structure. However, a high content of NMI above

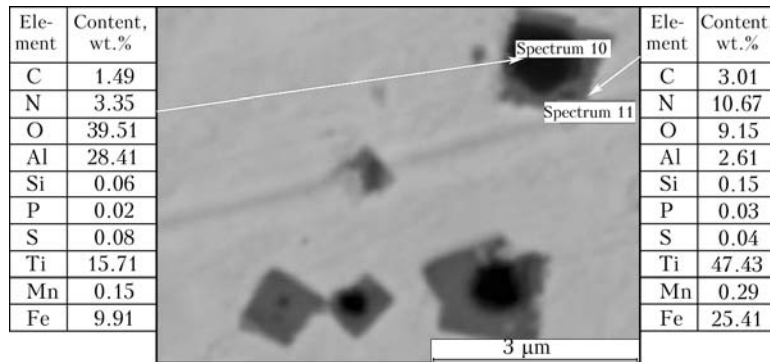


Figure 3. Morphology and composition of NMI less than 1.5 μm in size

Table 3. Amount of microstructure components (%) and mean size of ferritic grain in metal of the investigated welds

Weld designation	Acicular ferrite	Polygonal ferrite	Lower bainite	Upper bainite	Polyhedral ferrite	Ferritic grain size, μm
Ti-1	23.5	10.5	21.5	25.5	19	150
Ti-2	10	20	30	20	20	120
Ti-3	6	3.7	35	28	27.3	70
Ti-4	7	9	41	19.6	23.4	100
Ti-5	–	5.7	36.7	23.6	34	70
Ti-6	–	2	25.3	71.7	1	50

Table 4. Volume content of NMI, their size distribution, and results of calculation of distance between the λ particles

Weld designation	Volume content of inclusions, %	Content (%) / quantity (pcs) of inclusions in size ranges, μm					λ, μm
		< 0.3	0.5–1	1.25–2	2.25–3	> 3	
Ti-1	0.40	25 / 243	51 / 490	17 / 159	5 / 45	3 / 26	3.96
Ti-2	0.24	53 / 647	37 / 458	8 / 94	2 / 21	0.25 / 3	2.99
Ti-3	0.12	33 / 233	52 / 360	11 / 79	3 / 21	0.6 / 4	1.89
Ti-4	0.65	53 / 408	33 / 258	10 / 75	3 / 21	1.5 / 12	1.89
Ti-5	0.35	56 / 315	35 / 197	2 / 10	1.5 / 8	1.5 / 8	1.80
Ti-6	0.23	62 / 386	30 / 189	6 / 36	2 / 11	0.16 / 1	1.61



Table 5. Chemical composition of metal of the investigated welds, wt.%

Weld designation	C	Si	Mn	Ni	Mo	Ti	Zr	Al	S	P	O
Zr-1	0.055	0.480	1.53	0.31	0.38	0.022	0.001	0.013	0.013	0.016	0.035
Zr-2	0.054	0.522	1.67	0.30	0.37	0.015	0.007	0.014	0.014	0.018	0.037

Table 6. Mechanical properties of metal of the investigated welds

Weld designation	σ_t , MPa	$\sigma_{0.2}$, MPa	δ_5 , %	ψ , %	KCV, J/cm ² , at T, °C				
					20	-20	-40	-60	-70
Zr-1	736.6	667.0	20.8	61.6	181.3	147.9	96.7	65.9	54.8
Zr-2	740.7	650.2	20.2	62.3	198.8	141.7	94.2	87.5	80.6

1.5 μm in size along the grain boundaries shifts transformations to a high-temperature range. Therefore, mostly polygonal ferrite precipitated in the Ti-1 and Ti-2 weld metals (see Table 3), whereas the content of polyhedral ferrite was higher in structure of the Ti-3, Ti-4, Ti-5 and Ti-6 welds, where the content of oxide inclusions was lower.

Analysis of the obtained data allows a conclusion that increase in the content of the fine-grained structure can be achieved by varying the content of the fine carbide phase in structure of the weld metal (due to control of the metallurgical processes occurring in the slag-metal system). However, the welds have a low level of toughness because of formation of high-temperature morphological types of bainitic ferrite. To increase toughness and ductility of the weld metal it is necessary to achieve an increased content of the low-temperature types of ferrite in their structure due to refining of grains in the primary structure.

To refine the primary structure the weld pool should contain (by the beginning of solidification) refractory NMI in the form of a crystalline phase, which can serve as the γ-phase nucleation centres. Zirconium oxide ($T_{melt} = 2715\text{ °C}$) was added to the weld pool for this purpose. To increase stability of the austenitic phase, the welds were additionally alloyed with manganese. Chemical composition of the weld metal is given in Table 5, and mechanical properties — in Table 6.

Table 7 gives the data on composition of microstructure of the weld metal, which were obtained as a result of metallographic examinations, and Table 8 — the results of evaluation of microhardness of these structural components. Figure 4 shows histograms of the size distribution of NMI, and Table 9 gives the integrated chemical composition of NMI and amount of the 0.3–1.0 μm inclusions contained in them. It can be seen from analysis of the data that the character

Table 7. Amount of microstructure components (%) and mean size of ferritic grain in metal of the investigated welds

Weld designation	Martensite	Polygonal ferrite	Upper bainite	Lower bainite	MAC-phase	Ferritic grain size, μm
Zr-1	17	2	20	60	1	55
Zr-2	15	2	30	50	3	35

Table 8. Microhardness of structural components in metal of the investigated welds

Weld designation	Structural components	HV1, MPa	
		Unit values	Mean value
Zr-1	Lower bainite	205; 180; 187	190.7
	Upper bainite	232; 236; 254	241.2
	Martensite	490; 521; 545	519
Zr-2	Lower bainite	208; 187; 185	193.3
	Upper bainite	254; 236; 260	244
	Martensite	450; 457; 476	461

Table 9. Chemical composition, total content of NMI V_{NMI} , and content of fine inclusions $V_{0.3-1.0}$ in metal of the investigated welds

Weld designation	Chemical composition of NMI, wt.%							V_{NMI} , %	$V_{0.3-1.0}$, %
	O	Al	Si	S	Ti	Zr	Mn		
Zr-1	35.05	6.61	8.15	1.83	13.05	Traces	35.30	0.41	19.89
Zr-2	28.44	6.62	9.56	3.34	5.47	9.23	37.33	0.45	19.13

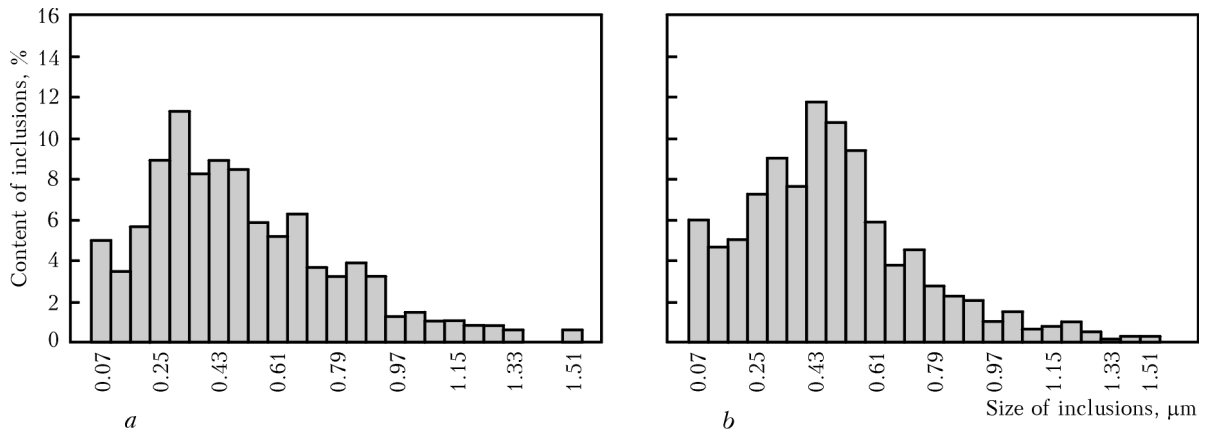


Figure 4. Size distribution of NMI in weld metals: *a* – Zr-1; *b* – Zr-2

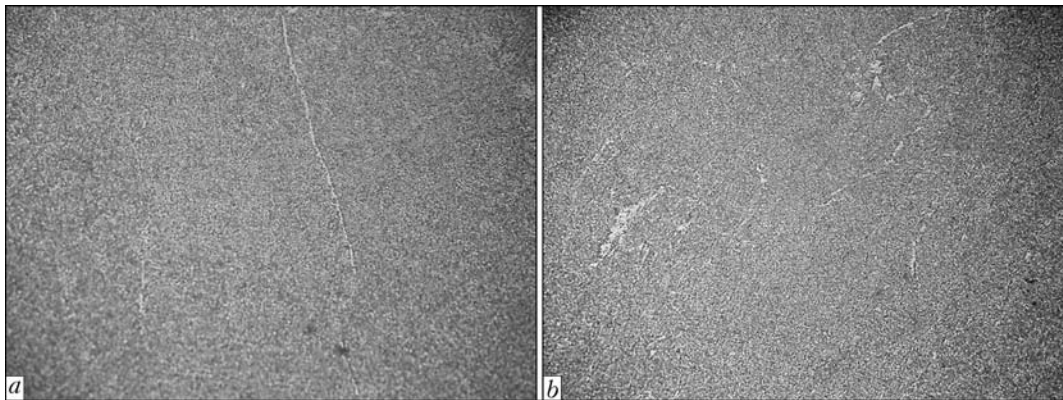


Figure 5. Microstructure ($\times 200$) of weld metal: *a* – Zr-1; *b* – Zr-2

of the size and chemical composition distribution of NMI in the Zr-1 and Zr-2 weld metals is similar and differs only in the titanium and zirconium contents. Metallographic examinations by using optical (Figure 5) and electron (Figure 6) microscopy were carried out to reveal the effect of such differences on the peculiarities of formation of microstructure of the weld metal.

As to the level of mechanical properties, the Zr-2 weld metal is characterised by a higher value of impact toughness at low temperatures, compared to the Zr-1 weld metal. This is provided by a combination of such hard component as lath martensite and a relatively soft phase presented by lower bainite contained in its structure.

It can be concluded from the results of measurement of microhardness of the structural components (see Table 8) that the low content of carbon in the Zr-1 and Zr-2 weld metals leads to decrease in its content in the lower bainite microstructure.

Sizes and numeric values of density of the inclusions in the microstructure of the weld metal were determined in the course of metallographic examinations. Each weld analysed to determine the content of the inclusions was examined by the optical and electron microscopy methods. 12 micrographs (frames) as a minimum were ob-

tained at a magnification from 500 to 6000. The mean size of oxide inclusions and numeric values of the density were in a range of about 250 to 650 nm and about $1.5 \cdot 10^{10}$ to $10.5 \cdot 10^{10} \text{ m}^{-2}$, respectively. In some cases, the mean size ranged from about 250 to about 550 nm.

Microstructure of the Zr-1 and Zr-2 weld metals contains oxide inclusions with a mean size of less than 1 μm . This distribution of the inclusions is achieved due to the presence of the oxide nuclei with a size of no more than 300 nm, which contain about 50 % of zirconium, titanium or their mixture, as well as due to the low content of oxygen. Formation of the sufficient amount of nuclei of the bainitic phase, fixation of the grain boundaries and deoxidation of the weld pool are provided by the corresponding contents of titanium and zirconium oxides, as well as deoxidisers in a composition of the welding flux.

The selected alloying system combined with a certain thermal cycle allows formation of the weld metal with a structure of the bainitic-martensitic type. It can be seen from comparison of the data shown in Figures 5 and 6 that structure of the Zr-1 and Zr-2 weld metals is in a range of the optimal compositions, which is marked in Figure 7.

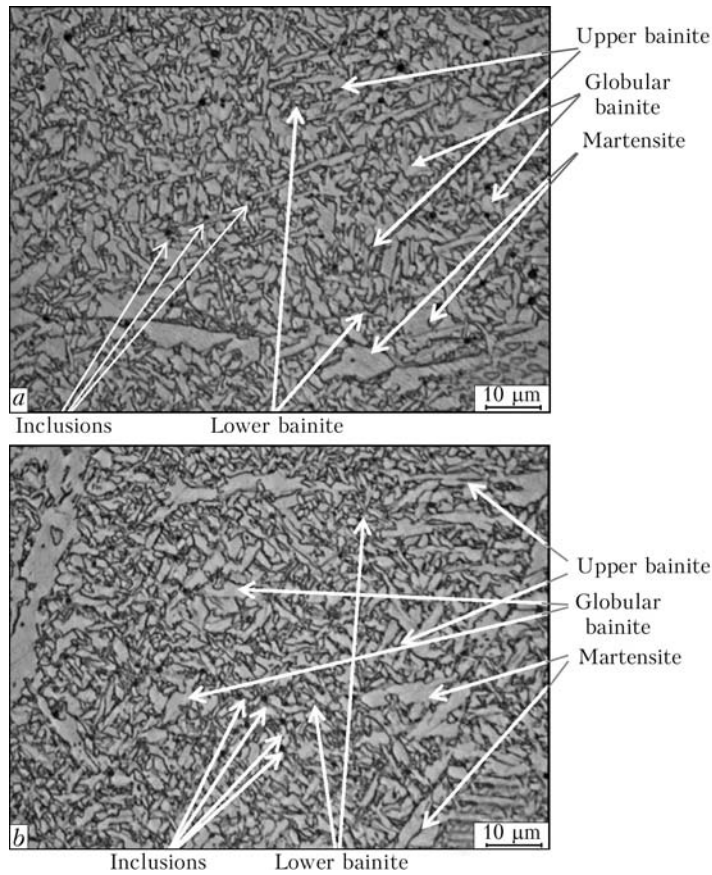


Figure 6. Microstructure of weld metal: *a* – Zr-1; *b* – Zr-2

The presence of martensite in the structure provides high strength properties of the weld metal. The values of ductility and toughness of metal depend on the content and morphology of such structural components as lower bainite and globular bainite.

Formation of lower bainite depends not only on the chemical composition of the weld metal and its cooling rate, but also on the chemical composition, size and value of the density of distribution of oxide inclusions in its composition. Application of the oxide metallurgy methods favours formation of a certain morphology of lower bainite and is a necessary condition for formation of microstructure of the weld metal on HSLA steels.

It was noted that the oxide inclusions more than 1 μm in diameter are inefficient for formation of lower bainite. Based on these results, the weld metal chemical composition and thermal welding cycle were selected so that they minimised formation of coarse oxide inclusions. Adding the certain amount of zirconium and titanium oxides to the weld pool exerts a marked effect on regulation of the size of the inclusions. This is also promoted by the limitation of the oxygen content of the weld metal to a level of less than 0.04 %, as well as by the use of strong deoxidisers, such as aluminium and silicon. Moreover, to

limit growth of the oxide inclusions, the value of the welding heat input should be chosen on the basis of a permissible range of metal cooling rates v_{cool} (see Figure 7). The mean size of the oxide inclusions under these conditions ranges from 250 to 500 nm.

The high density of distribution of the 0.3–1.0 μm inclusions containing titanium or zirconium oxides leads to formation of the bainitic structure, whereas the decreased content of carb-

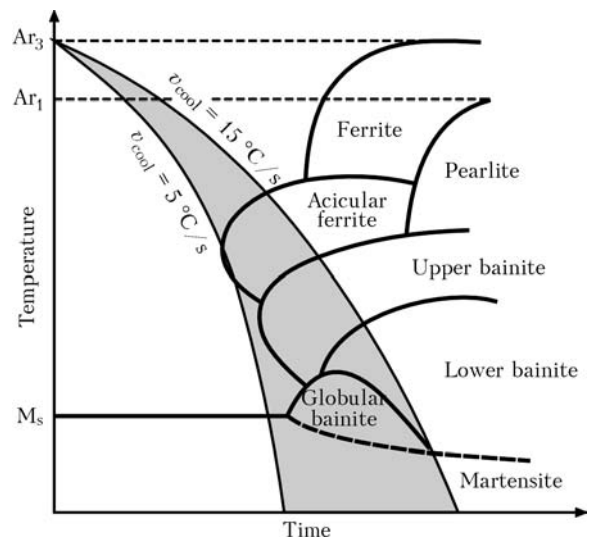


Figure 7. Diagram of structural transformations during continuous cooling of metal of the investigated welds

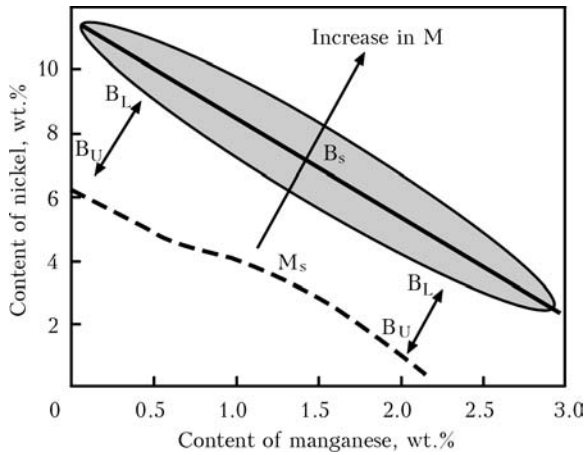


Figure 8. Diagram of the effect of alloying on the temperature of start of bainitic B_s and martensitic M_s transformations, and range of formation of upper B_U and lower B_L bainite and martensite M in microstructure of HSLA steels [12]

on in metal and the narrow range of bainitic transformations, which is determined by the value of the B_s - M_s temperature range (Figure 8), limit the probability of formation of the upper bainite microstructure.

In a general case, the solid oxides are worse wetted with metal than the liquid ones. Hence, they can be more readily entrapped by growing dendrites. It is this fact that can explain behaviour of the oxide inclusions containing titanium or zirconium.

By analysing the results of metallographic examinations, we can note differences in morphology of these inclusions. While the inclusions containing titanium oxides have a rounded shape (Figure 9), the inclusions containing zirconium oxides have an irregular shape formation in their inner part (Figure 10). This confirms an assumption that at the moment of growth of dendrites the inclusions are in the form of a solid phase.

The inclusions containing titanium compounds have, as a rule, manganese and silicon oxides in their composition. It can be seen from the constitutional diagram of the MnO - SiO_2 - MnO - TiO_2 system (Figure 11) that the melting temperature of such inclusions is lower than the temperature of solidification of low-alloy steels. The constitutional diagram of the MnO - SiO_2 - ZrO_2 system (Figure 12) shows that even at a content of up to 50 % of manganese silicates in the oxide phase, a non-metallic inclusion containing zirconium oxide can remain solid at temperatures above 1500 °C. Such inclusions are capable of blocking the growth of dendrites and affecting the grain size in the primary structure of the weld metal.

Fine refractory zirconium oxides up to 500 nm in size are sorbed by the boundaries of growing

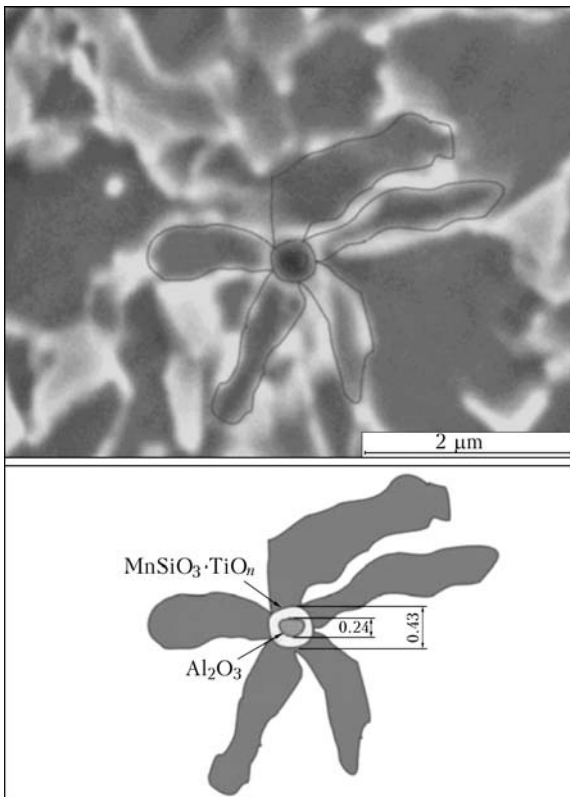


Figure 9. Morphology of non-metallic inclusion containing titanium oxide

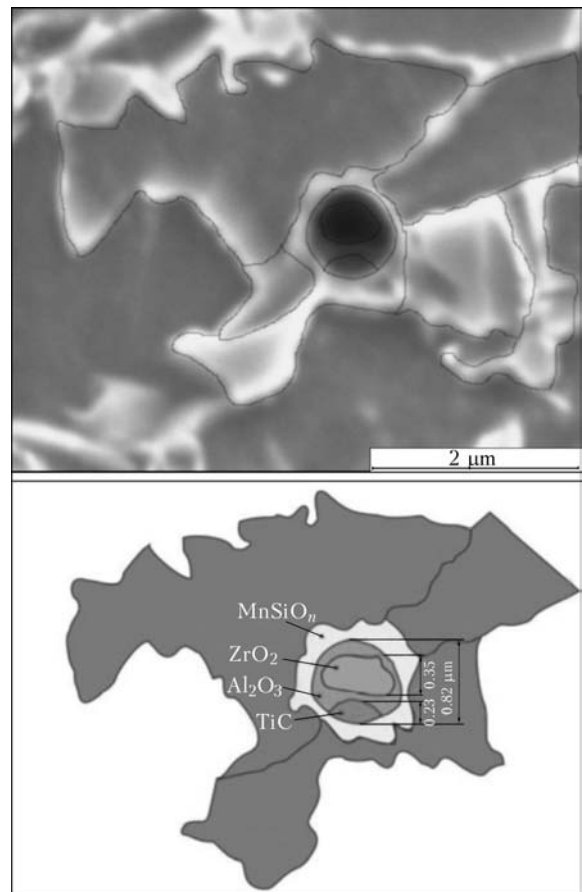


Figure 10. Morphology of zirconium oxide based non-metallic inclusion

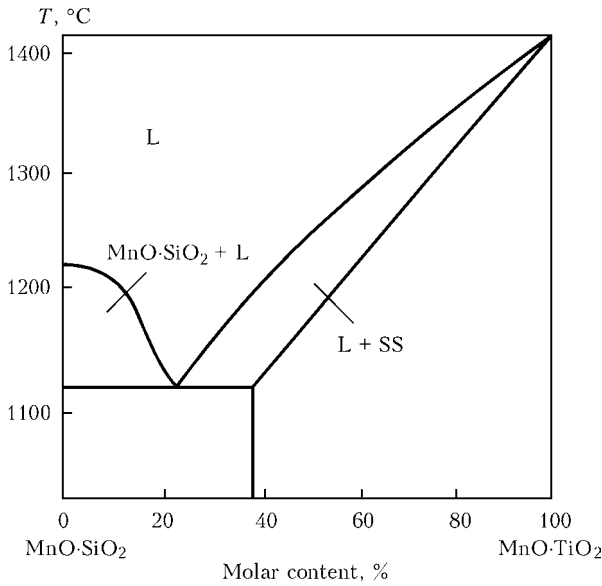


Figure 11. Constitutional diagram of the MnO-SiO₂-MnO-TiO₂ system

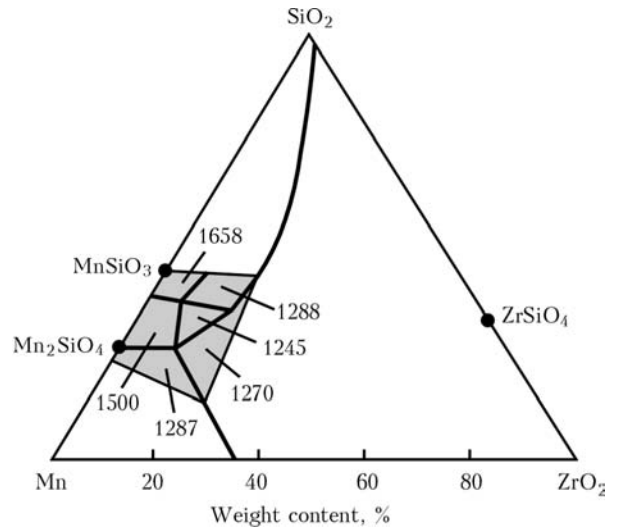


Figure 12. Constitutional diagram of the MnO-SiO₂-ZrO₂ system (numbers in the diagram – values of melting temperatures of the compounds)

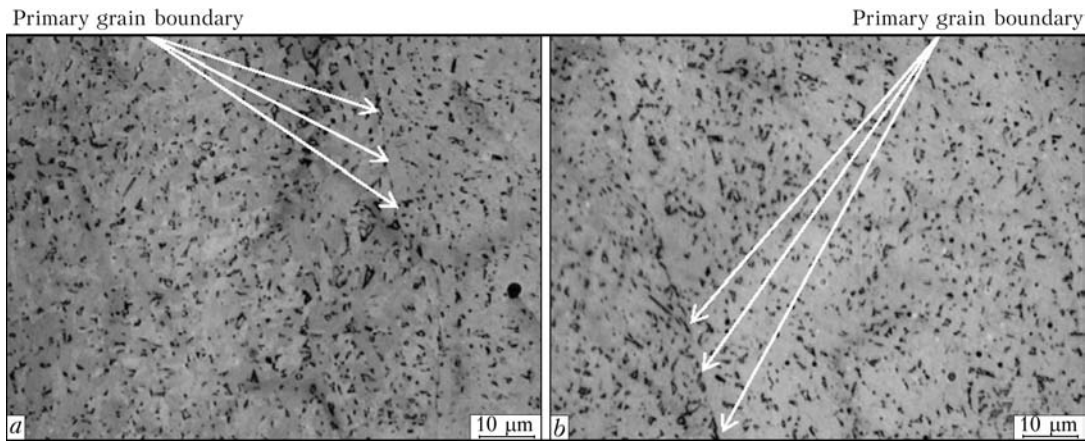


Figure 13. Character of precipitation of second phase particles at the boundary of primary grains in weld metal specimens: a – Zr-1; b – Zr-2

crystals, this leading to fixation of the grain boundaries. The inclusions exerting this effect are very fine and, therefore, are not the efficient centres of initiation of fracture in the inter-phase plane.

To check this assumption, additional metallographic examinations of specimens of the Zr-1 and Zr-2 weld metals were carried out in order to reveal the primary structure grain boundaries. Transverse sections of the welded joints were etched in a boiling solution of sodium picrate, and then examined by using optical microscope «Neophot 30». Figure 13, *a*, presents a photo of the typical structures, which shows precipitates of the second phase particles at the primary grain boundary in the Zr-1 weld metal in the form of a continuous chain. The second phase particles precipitate also along the primary grain boundary in structure of the Zr-2 weld metal (Figure 13, *b*), but these precipitates do not have a character of the continuous chain. Differences in the char-

acter of precipitation of the second phase at the boundary of growing dendrites affect the size of the secondary structure grains (see Table 7) and mechanical properties of the weld metal (see Table 6).

It can be seen from the examination data that NMI are a necessary component of the weld metal in welding of HSLA steels. To provide the microstructure characterised by a combination of high values of strength, ductility and toughness, it is necessary to form inclusions of a certain composition, size and distribution density in the weld metal.

Conclusions

1. The possibility of using oxide metallurgy approaches was investigated, providing for control of the amount, distribution and morphology of the inclusions in metal melts affecting the conditions of formation of the weld metal microstructure.



2. The presence of the NMI up to 1 μm in size containing titanium oxides in the weld metal on HSLA steels provides formation of a tough ferritic-bainitic structure with an increased content of acicular ferrite.

3. The content of the fine secondary structure can be increased by varying the content of the fine carbide phase in structure of the weld metal. However, because of formation of high-temperature morphological types of bainitic ferrite, the welds in this case have a low level of toughness.

4. The high density of distribution of the 0.3–1.0 μm inclusions containing titanium or zirconium oxides leads to formation of the bainitic structure, whereas the decreased content of carbon in metal and narrowing of the bainitic transformation range limit the probability of formation of the upper bainite microstructure.

5. Fine refractory zirconium oxides up to 500 nm in size are sorbed at the boundaries of growing crystals, this leading to fixation of the grain boundaries. The differences in the character of precipitation of the second phase at the boundary of growing dendrites affect the size of the secondary structure grains and mechanical properties of the weld metal.

6. To provide the microstructure characterised by a combination of high values of strength, ductility and toughness, it is necessary to form inclusions of a certain composition, size and distribution density in the weld metal. This can be achieved by using the oxide metallurgy methods providing for addition of a certain amount of refractory inclusions into the weld pool, limitation of the content of oxygen in it, and selection of the deoxidation system, as well as determination of the required temperature range of intermediate transformations based on the TTT-diagrams and welding thermal cycle.

1. Fairchild, D.P., Macia, M.L. (2003) Girth welding development for X120 linepipe. In: *Proc. of 13th Int. Offshore and Polar Engineering Conf.* (Honolulu, Hawaii, 25–30 May, 2003), 26–35.
2. Dhua, S.K., Mukerjee, D., Sarma, D.S. (2002) Weldability and microstructural aspects of shielded metal arc welded HSLA-100 steel plates. *ISIJ Int.*, **42**(3), 290–298.
3. Grong, O., Kolbeinsen, L., van der Eijk, C. et al. (2006) Microstructure control of steels through dispersoid metallurgy using novel grain refining alloys. *Ibid.*, **46**, 824–831.
4. Takamura, J., Mizoguchi, S. (1990) Roles of oxides in steels performance – Metallurgy of oxides in steels. *Ibid.*, **1**, 591–597.
5. Lee, T.K., Kim, H.J., Kang, B.Y. et al. (2000) Effect of inclusion size on nucleation of acicular ferrite in welds. *Ibid.*, **40**(1), 1260–1268.
6. Pokhodnya, I.K., Golovko, V.V., Denisenko, A.V. et al. (1999) Effect of oxygen on formation of acicular ferrite in low-alloy weld metal (Review). *Avtomatich. Svarka*, **2**, 3–10, 20.
7. Li, H.G., Zheng, S.B., Xie, S.J. et al. (2009) Influence of liquid steel cooling rate during directional solidification on titanium oxide precipitation. *Ironmaking and Steelmaking*, **36**(1), 29–32.
8. Kikuchi, N., Nabeshima, S., Yamashita, T. et al. (2011) Microstructure refinement in low carbon high manganese steels through Ti-deoxidation, characterization and effect of secondary deoxidation particles. *ISIJ Int.*, **51**(12), 2019–2028.
9. Sarma, D.S., Karasev, A.V., Jonsson, P.G. (2009) On role of non-metallic inclusions in the nucleation of acicular ferrite in steels. *Ibid.*, **46**(6), 1063–1074.
10. Grigorenko, G.M., Golovko, V.V., Kostin, V.A. et al. (2005) Effect of microstructural factors on sensitivity of welds with ultra-low carbon content to brittle fracture. *The Paton Welding J.*, **2**, 2–10.
11. Golovko, V.V., Kostin, V.A., Grigorenko, G.M. (2011) Peculiarities of the influence of complex alloying on structure formation and mechanical properties of welds on low-alloyed high-strength steels. *The Paton Welding J.*, **7**, 11–17.
12. Keehan, E., Karlsson, L., Andren, H.-O. et al. (2006) New developments with C-Mn-Ni high-strength steel weld metals. Pt A: Microstructure. *Welding J.*, **9**, 200–210.

Received 27.03.2013